Process Analysis of Pressurized Oxy-Coal Power Cycle for Carbon Capture Application Integrated with Liquid Air Power Generation and Binary Cycle Engines

Mathew Aneke, Meihong Wang*

Process and Energy Systems Engineering Group, School of Engineering, University of Hull, HU6 7RX, United Kingdom

*Corresponding author: Tel: +44 1482 466688; Fax: +44 1482 466664; Email: Meihong.Wang@hull.ac.uk

Abstract

In this paper, the thermodynamic advantage of integrating liquid air power generation (LAPG) process and binary cycle waste heat recovery technology to a standalone pressurized oxy-coal combustion supercritical steam power generation cycle is investigated through modeling and simulation using Aspen Plus® simulation software version 8.4. The study shows that the integration of LAPG process and the use of binary cycle heat engine which convert waste heat from compressor exhaust to electricity, in a standalone pressurized oxy-coal combustion supercritical steam power generation cycle improves the thermodynamic efficiency of the pressurized oxy-coal process. The analysis indicates that such integration can give about 12 – 15% increase in thermodynamic efficiency when compared with a standalone pressurized oxy-coal process with or without CO_2 capture. It was also found that in a pressurised oxy-coal process, it is better to pump the liquid oxygen from the cryogenic ASU to a very high pressure prior to vapourization in the cryogenic ASU main heat exchanger and subsequently expand the gaseous oxygen to the required combustor pressure than either compressing the atmospheric gaseous oxygen produced from the cryogenic ASU directly to the combustor pressure or pumping the liquid oxygen to the combustor pressure prior to vapourization in the cryogenic ASU main heat exchanger. The power generated from the compressor heat in the flue gas purification, carbon capture and compression unit using binary cycle heat engine was also found to offset about 65% of the power consumed in the flue gas cleaning and compression process.

The work presented here shows that there is a synergistic and thermodynamic advantage of utilizing the nitrogen-rich stream from the cryogenic ASU of an oxy-fuel power generation process for power generation instead of discarding it as a waste stream.

Keywords: Liquid air energy storage; Pressurised Oxy-coal combustion; Air separation unit; Process integration; Process simulation

1. Introduction

1.1 Coal-fired power generation and Post-combustion Carbon Capture

The global climate change resulting from CO_2 and other greenhouse gas emissions has become one of the greatest environmental threats of our time. Reduction in CO_2 emission especially from coal-fired power plants has been the mainstay of many researches on climate change mitigation. Studies show that a one percent point improvement in the efficiency of a conventional pulverised coal combustion power plant can result in a 2 – 3% reduction in CO_2 emission (WCA, 2014).

Despite the historical tightening of emission constraints from coal-fired power plants, its use for power generation has been on the increase mainly due to its availability, cost and the ever increasing global energy demand ((IEA, 2013, IEA, 2012, IEA, 2011). This shows that coal will continuously play a major role in meeting the global energy need. However, the success will depend on the development of technologies to control pollution and CO_2 emissions from such plants (Ciferno et al., 2000) especially now that CO_2 is becoming regulated in the US and Europe.

Carbon capture and sequestration (CCS) technologies have been in development for over a decade (Hagi et al., 2013) and is required to provide a long term solution by virtually eliminating CO_2 emission from coal-fired power plants. One of the CCS technologies which has been under investigation for decades now is the post-combustion process. Post-combustion technology involves capturing the CO_2 contained in the flue gas after the combustion process. Unlike the pre-combustion technology, this technology can easily be added to existing fossil fuel power plants for CO_2 capture. The efficiency of this technology largely depends on the concentration of the CO_2 in the flue gas. The major barriers opposing the commercialisation of this technology include: (a) high capital and operation cost; (b) steam consumption for solvent regeneration (Ciferno et al., 2000).

1.2 Oxy-fuel combustion and its recent development

Conventional coal based power plants produces flue gas with up to 10 - 15 vol% CO_2 (Ciferno et al., 2000, Hong et al., 2009). The low CO_2 content of the flue gas makes the capture operation energy intensive. One way of improving the CO_2 concentration in the flue gas is by using pure oxygen in the combustion process instead of air. The replacement of air with oxygen otherwise known as oxy-fuel combustion helps to produce a flue gas that contains mainly CO_2 and water vapour (Hong et al., 2009, Hu and Yan, 2011, Roy and Bhattacharya, 2013), which can easily be separated.

Studies had shown that there are more potential in pressurized oxy-fuel process compared to atmospheric oxy-fuel combustion power cycles. ENEL work in the area of pressurized oxy-fuel combustion using a novel pressurized oxy-combustion technology, known as the Isotherm Pwr® technology shows an increased heat transfer rates on the heat recovery steam generator (HRSG) compared to atmospheric oxy-combustion process (Zheng, 2011, Barbucci, 2008). In the Isotherm Pwr® process, combustion takes place at elevated pressures and at 1400 – 1600 ^{o}C.

However, one big challenge facing oxy-fuel process is the high energy requirement of the cryogenic air separation unit (ASU) which is currently the only mature air separation technology that can produce high purity, high tonnage oxygen required by the power plant. Thus improving the energy efficiency of the ASU is paramount to the success of oxy-fuel combustion process.

Several studies have been carried out on how to reduce the energy demand of cryogenic ASU for oxy-fuel combustion application. Some of the studies include:(1) improving the energy efficiency of heat exchangers and compressors and (2) the use of control system with real time optimization capability (Castle, 2002, Rübberdt, 2009), (3) use of self-heat recuperation process (Kansha et al., 2011), (4) pumping the liquid oxygen produced to a very high pressure prior to vaporization and expansion to the required process pressure (Manenti et al., 2013), (5) recovery of the compressor heat using organic Rankine cycle system (Aneke and Wang, 2015b, Aneke and Wang, 2015a).

1.3 Liquid air power generation and Motivation for process integration

The recent breakthrough in liquid air power generation (LAPG) provides a new synergistic advantage for minimizing the high energy concern associated with oxy-fuel combustion of fossil fuels through integration with other processes. In a typical oxy-fuel combustion process, high tonnage gaseous nitrogen rich stream which contains about 80 mol% - 95 mol% nitrogen is produced together with the 95 mol% oxygen required for the oxy-fuel process. Presently, this gaseous nitrogen rich stream is discarded as waste since there is usually no need for nitrogen on site. However, demonstration plant studies had shown that this waste gas stream is an ideal working fluid for LAPG (Strahan, 2013). Thus, LAPG could be annexed to an oxy-fuel combustion process in order to improve both the overall power output and energy efficiency of the process. More heat integration opportunities could be possible depending on the plant configuration.

1.4 Novel contributions of this study and outline of this paper

In this study, the thermodynamic advantage of integrating LAPG and binary cycle waste heat recovery heat engines to pressurized oxy-coal combustion with supercritical steam power cycle will be investigated through modeling and simulation using Aspen Plus® version 8.4 simulation software. The entire process will be analysed to evaluate the impact of integrating the aforementioned process to the thermodynamic efficiency of a pressurized oxy-coal supercritical steam power cycle process which is used as the base case scenario. Different process scenarios will be investigated with/without carbon capture consideration. To the knowledge of the authors, this is the only work that has introduced the concept of utilizing the nitrogen rich stream from the ASU of an oxy-fuel combustion process for power generation instead of the current practice where it is discarded as a waste stream.

This paper is presented in five sections. The first section is the introduction and covers the carbon capture technologies, the liquid air power generation technology and the synergistic advantage of integrating oxy-fuel technology with liquid air power generation technology which is the underlining novelty of the paper. In the second section, the description of the different processes is presented while in section three, the Aspen simulation of the overall process is presented together with the modeling parameters and process efficiency definitions and equations. In section four, the results from the process simulation were presented and discussed while in section five, the conclusions drawn from the study carried out is presented.

2. Process Description

Figure 1 shows the process flow diagram of the pressurized oxy-coal combustion supercritical steam power cycle integrated with liquid air power generation and binary cycle heat engines proposed in this study. The process shown in Figure 1 consists of eight primary units: 1) Cryogenic ASU; 2) Pressurized oxy-coal combustor unit; 3) Steam generation unit; 4) Supercritical steam power generation unit; 5) Air liquefaction unit; 6) LAPG unit; 7) Flue gas purification, Carbon dioxide capture and compression unit; 8) Binary cycle waste heat recovery units.

The pressurized oxy-coal combustor, steam generation unit and supercritical steam power generation unit were adapted from Hong et al., (2009) and Zheng (2011). The cryogenic ASU and heat recovery using binary cycles were based on the previous work of the authors (Aneke et al., 2012, Aneke and Wang, 2015a, Aneke et al., 2011b), flue gas purification, carbon dioxide capture and compression unit were adapted from White et. al., (2009) while the air liquefaction and LAPG unit were adapted from a demonstration plant study carried out by the authors.

An overview of the process flow diagram shown in Figure 1 is as follows: the 10 bar pulverised coal slurry (stream 5) is first dried at the entrance to the combustor. This is followed by the decomposition of the coal into its constituents based on the properties of coal as shown in Table 1.

Figure 1: Overall Process Flow Diagram of the Pressurized Oxy-coal Power Cycle for Carbon Capture Application Integrated with LAPG and Binary Cycle Engine

Table 1: Properties of coal used in the simulation (adapted from (Hu and Yan, 2011))

The pressurized coal is burnt with 95.68 mol% oxygen from the cryogenic ASU (stream 4) and a portion of the recycled flue gas, (stream 10) which helps to maintain the combustion temperature at 1550 ^{o}C. A second portion of the flue gas recycle (stream 9) is used to control the temperature at the heat recovery steam generator (HRSG) inlet, which is kept close to 800 ^{o}C to avoid slagging (Zheng, 2011) and also minimize hot corrosion and oxidation (Hong et al., 2009). The hot temperature-controlled flue gas (stream 6) is passed through the HRSG where it is used to generate supercritical steam used in the supercritical steam power generation unit.

The HRSG consists of two superheaters, a once-through boiler and an economizer. The steam reaches the supercritical state of 600 ^{o}C at 250 bar before being delivered to high pressure turbine (HPT) of the supercritical steam power generation unit. The superheater also acts as a re-heater to generate two reheat subcritical steam of 620 ^{o}C at 50 bar and 10 bar for the intermediate pressure turbine (IPT) and the low pressure turbine (LPT) respectively. Due to the presence of SO_x and NO_x in the flue gas, flue gas from the exit of the HRSG must be maintained at a temperature higher than the acid dew point. This is maintained at 239 ^{o}C in this present work. The remaining flue gas after the recycle is compressed to 15 bar and sent to the flue gas purification unit where water, SO_x, NO_x and inert gases are removed from the flue gas to achieve about 95.35 mol% CO_2 which is compressed to 110 bar (stream 52) and sent to the storage facility.

The nitrogen rich gas stream gas (stream 3) from the ASU unit is compressed and liquefied to produce the working fluid for the LAPG unit. The liquid nitrogen-rich stream otherwise known as the liquid air is pumped to a pressure of 120 bar (stream 33) vaporized using heat extracted from the supercritical steam power generation unit and expanded in a 4 stage turbine and reheat arrangement in the LAPG unit to produce power.

The compressor heat from the intercooler and after-cooler heat exchangers in the cryogenic ASU unit, LAPG unit, the flue gas purification and the CO_2 compression unit were utilized for power generation using binary cycle heat engine which uses R134a as the working fluid. The detailed description of each of the process unit is as given below.

2.1 Cryogenic Air Separation Unit

As aforementioned, oxy-coal combustion process uses oxygen at >95mol% purity instead of air for combustion operation. For the pressurized oxy-coal combustion process developed in this study, the combustion pressure is assumed to be 10 bar while the combustion chamber is maintained at 1550 ^{o}C using a mixture of oxygen and flue gas recycle. The oxygen used in the combustion chamber is produced from a cryogenic ASU and should be supplied at a pressure of 10 bar.

The process flow diagram of the cryogenic ASU for the specialist application proposed in this work is shown in Figure 2. Unlike the conventional ASU, the ASU proposed in this work makes use of only 2 columns to produce nitrogen-rich gaseous stream and 95.68 mol% liquid oxygen stream since there is no need for pure nitrogen and argon stream. The nitrogen-rich gaseous stream and the liquid oxygen stream exchanges heat with the in-coming air stream in the main heat exchanger in order to obtain an all gaseous product.

In the process, atmospheric air is filtered, cleaned and compressed in a 3 stage compressor with inter-cooling to a pressure of 6.35 bar. The compressed air is split into two, cooled and partially liquefied against leaving product streams (gaseous nitrogen-rich stream and liquid oxygen-rich stream (95.68 mol% purity)). One of the streams is sent to the high pressure column (HPC) where nitrogen is separated at a pressure of about 6 bar. The other stream is expanded in an air expander to a pressure of about 1.2 bar and sent to the low pressure column (LPC). The top nitrogen product from the HPC is condensed against the boiling oxygen in the reboiler of the LPC, before being depressurized and sent to the top of the LPC. The bottom liquid product form the HPC is also sent to the LPC after been depressurized in the JT valve. In the LPC, gaseous nitrogen-rich stream which contains about 94.54 mol% nitrogen leaves through the top of the column while the liquid oxygen rich stream (95.68 mol% oxygen) which is required for the oxy-coal combustion leaves through the bottom of the column.

It is proposed in this work that the liquid oxygen produced in the cryogenic ASU be pumped to about 200 bar prior to vapourization in the main heat exchanger against in-coming air feed to the system. The high pressure gaseous oxygen from the main heat exchanger will then be expanded in the turbine to 10 bar (required combustion pressure), thus generating extra energy.

Figure 2: Process Flow Diagram of Cryogenic ASU

2.2 Pressurized Coal Combustion, Steam Generation Unit and Supercritical Steam Power Generation Unit

The pressurized coal combustor process is based on the novel Isotherm Pwr® technology developed by ENEL (Zheng, 2011, Hong, 2009). The combustion is assumed to take place at a pressure of 10 bar and temperature of 1550 ^{o}C. In the process, wet coal is first dried and burnt with a mixture of 95.68 mol% oxygen and 23.4% (by mass) recycled flue gas in order to maintain the temperature of the combustor at 1550 ^{o}C. The exit flue gas from the combustion chamber is mixed with about 66.6% of the recycled flue gas in order to maintain the temperature to the HRSG at about 730 ^{o}C.

The supercritical steam generation unit otherwise known as the HRSG comprises of two superheaters, a once-through boiler and an economizer. The heating in the steam generation unit is provided by the temperature controlled flue gas at 730 ^{o}C in a counter-current flow arrangement. The flue gas enters the first superheat of the HRSG at about 730 ^{o}C and is used to generate a supercritical steam at 600 ^{o}C and 250 bar and a subcritical steam (reheat stream) at 620 ^{o}C and 50 bar. The effluent flue gas from the first superheater is sent to the second superheater where is it used to further generate a subcritical steam (reheat stream) at 620 ^{o}C and 10 bar. From the second superheater, the flue gas enters the once-through boiler and the economiser where it is used to preheat and generate steam respectively before exiting the HRSG at about 239 ^{o}C.

The steam power generation unit comprises of a supercritical Rankine cycle. The supercritical steam at 600 ^{o}C and 250 bar generated in the first superheater of the HRSG enters into the high pressure turbine (HPT). The steam is expanded in the HPT to produce power. Part of the steam from the HPT is also injected into the pressurized combustor. Part of the exit steam from the HPT is reheated in the HRSG and used to provide steam for the intermediate pressure turbine (IPT) while the remaining is sent to the deaerator via a heat exchanger arrangement which is used to preheat the feed water system. The reheated steam at 620 ^{o}C and 50 bar is expanded in the IPT to produce more power. Steam bleeding from the IPT is also used to preheat the feed water from the deaerator. Part of the exit steam from the IPT is returned to the HRSG and reheated to 620 ^{o}C before being sent to the low pressure turbine (LPT) while the remaining steam is sent to the deaerator. In the LPT, the steam is expanded for power generation. The exit steam from the LPT is condensed using cooling water at 25 ^{o}C. The condensed stream is preheated using heat from the water used to cool the combustion chamber wall. The combustor is assumed to lose 2% of the lower heating value of the coal to the water-cooled wall of the combustor (Hong et al., 2009). The preheated stream is sent to the deaerator where the whole liquid stream together with the makeup water is collected and pumped back into the HRSG to complete the steam cycle. The process flow diagram for these units is shown in Figure 3.

Figure: 3 Process Flow Diagram of Pressurized Combustor Unit, Steam Generation Unit and Supercritical Steam Power Generation Unit

2.3 Air Liquefaction Unit

Figure 4 shows the liquefaction unit where the nitrogen-rich (94.54 mol %) gaseous stream from the cryogenic ASU is liquefied to produce liquid nitrogen-rich stream otherwise known as liquid air. The process is based on the principle of Claude liquefaction cycle. The nitrogen-rich gas stream from the ASU is compressed in a 3 stage compressor with intercooler and after-cooler arrangement. The compressed gaseous stream is further compressed using a compressor joined to the shaft of an expander. The compressed gas is cooled with water and further cooled in the cold box with cryogenic gaseous stream from the expander outlet. The cold gaseous stream is expanded in the expander and the pressure dropped to produce a two phase stream (liquid and gas). The gaseous stream is used to cool incoming stream in the cold box while the liquid phase is sent to the cryogenic tank.

Figure 4: Process Flow Diagram of Air Liquefaction Unit

2.4 Liquid Air Power Generation (LAPG) Unit

In this unit, the liquid air in the cryogenic tank is pumped to about 120 bar and vapourized indirectly using a hot water loop which collects heat from the steam power generation unit.

The vapourized air is expanded in a series of 4 stage expanders with inter-heaters to produce power (Figure 5).

Figure 5: Liquid Air Power Generation Unit

2.5 Flue gas purification, carbon dioxide capture and compression unit

After recycling of about 90% of the flue gas leaving the HRSG, the remaining flue gas is cleaned to remove the NO_x, SO_x and the inert gases. The cleaning of the flue gas starts with an increase in the pressure of the flue gas to 15 bar. After the compression operation, direct contact scrubbing was used to cool the flue gas product as well as condense water vapour present in the flue gas and remove residual ash particles and highly soluble SO_3.

The removal of SO_2 involves the reaction of NO_2 with SO_2 to form sulphuric acid.

$$NO_2 + SO_2 + H_2O \longrightarrow NO + H_2SO_4 \qquad (1)$$

This reaction is fast and so is considered to be equilibrium limited. Since most of the NO_x in the flue gas occurs as NO, the NO would have to be converted to NO_2 to allow equation 1 to proceed. The conversion of NO to NO_2 occurs as

$$NO + 1/2O_2 \longrightarrow NO_2 \qquad (2)$$

Reaction 2 is a third order reaction with reaction rate given as (White et al., 2009)

$$d[NO2]/dt = 2k[NO]^2.[O2] \qquad (3)$$

where k, in $l^2\ mol^{-2}\ s^{-1}$ is $1200 \times 10^{230/T}$ where T is in Kelvin (White et al., 2009, Tsukahara et al., 1999).

Since the rate is proportional to pressure to the 3rd power, it is assumed that the reaction rate will become significant at the pressure of 15 bars and low temperature obtained after scrubbing.

After the removal of SO_2, the flue gas is compressed to about 30 bar, dried and then purified further to remove the inert gases such as nitrogen and argon using low temperature processing. In the process, the impure flue gas is cooled in HX1 and HX2 against evaporating lower pressure liquid CO_2 streams to a temperature of -55 ^oC, which is close to its triple point. The inert stream leaving the cold equipment at about 30 bars is further heated and expanded to produce power while the 95.35 mol% pure CO_2 streams leaving the cold equipment are compressed adiabatically in a second stage of CO_2 compression to a pressure of 110 bars. The process flow diagram is shown in Figure 6.

Figure 6: Process Flow Diagram of flue gas Cleaning, CO_2 purification and compression unit

2.6 Binary Cycle/Organic Rankine Cycle (ORC) Waste Heat Recovery Unit

Because there is no need for further heat integration in the process, the ORC unit is used to convert the waste heat from the compressor exhausts to electricity by acting as the compressor intercooler and after cooler system(Aneke and Wang, 2015b). In the ORC unit, the waste heat from the compressor exhaust is used to preheat and vapourise an organic working fluid in the evaporator. The vapourised organic fluid from the evaporator passes through the turbine where it is expands to produce work which turns the shaft connected to the generator to produce electricity (Aneke et al., 2012). The process flow diagram of a typical ORC system is shown in Figure 7. The system is used in all the compressors as shown in Figures 2 to 6 to compressor heat to electricity. The process uses R134a as the working fluid (Aneke et al., 2012, Aneke et al., 2011a).

Figure 7: Process Flow Diagram of Organic Rankine Cycle

The individual process flow diagrams presented in this work are linked to each other using alphabets from A to J.

3. Aspen Plus® Simulation of the Overall Process

The overall model of the process was developed using Aspen Plus® v8.4. Aspen is modular mode steady state simulation software. It contains modules of unit operations (like heat exchangers, reactors, turbine, flash, pumps etc.) used in the development of the model of the entire process described in this paper. The model equations used to model the individual unit operations and the physical property calculator used to model the process stream property in Aspen were standard equations. Due to the complexity of the flowsheet and in order to improve the convergence and the simulation time, the entire flowsheet of the process as represented in Figure 1 is split into five main sub-processes: 1) pressurised coal combustion, steam generation and supercritical steam power generation unit, 2) cryogenic air separation unit, 3) nitrogen-rich stream air liquefaction and liquid air power generation unit, 4) flue gas purification, carbon capture and CO_2 compression unit and 5) binary cycle heat engine units. The sub-processes were simulated individually and the results transferred to the appropriate sub-process as inputs.

Coal is modeled as a non-conventional component using the ultimate and proximate analysis (Table 1). The coal combustor in this work is modeled using the RGibbs reactor while the coal decomposition is modeled using RYield reactor together with the proximate and ultimate analysis of the coal. The fluid property of the overall process is modeled using Peng Robinson while the steam properties is modeled using STEAM-TA (ASME 1967 steam table correlations). The SO_2 removal is modeled using RadFrac column with chemical reaction. The pressure drop in the heat exchangers is assumed to be negligible. The simulation parameter for the overall process is given in Table 2.

Table 2: Process Simulation Parameters

In order to investigate the contribution of each of the process unit to the efficiency of a standalone pressurised oxy-coal process with/without carbon capture, different kinds of process efficiencies were evaluated and analysed in this study. The first three process scenarios show the impact of how gaseous oxygen is supplied from the cryogenic ASU on the efficiency of the pressurized oxy-coal process. Three different methods of supplying pressurized gaseous oxygen to the combustion chamber were investigated in the paper. The first is by pressurizing the gaseous oxygen produced in the cryogenic ASU to combustion chamber pressure of 10 bar (Case 1), the second is pumping the liquid oxygen produced in the cryogenic ASU to 10 bar before vapourizing it in the ASU main heat exchanger (Case 2) while the third is by pumping the liquid oxygen to 200 bar before vapourizing it in the ASU main heat exchanger and then expanding the high pressure gaseous oxygen to the required combustion chamber pressure of 10 bar (Case 3) thus producing extra power from the expander.

The baseline process scenario also known as the standalone pressurized oxy-coal process (Case 1) is regarded as the configuration where there is no heat recovery from compressors of the cryogenic ASU unit, no integration with liquid air power generation unit and where gaseous oxygen product from the cryogenic ASU is compressed to the combustor pressure of 10 bars before being mixed with the recycle flue gas stream going into the combustion chamber. As aforementioned, other alternatives include: pumping the liquid oxygen produced in the LPC of the cryogenic ASU to 10 bars prior to vapourization in the main ASU heat exchanger and subsequent mixing with the recycled flue gas into the combustor (Case 2) and pumping to 200 bar prior to vapourization and expanding the gaseous oxygen to 10 bars before been sent to the combustor with the recycled flue gas (Case 3). All the process scenarios were evaluated with/without carbon capture.

For processes without carbon capture, the efficiencies are defined as follows:

For Case 1, the efficiency of the standalone pressurised oxy-coal combustion process with supercritical steam power cycle and 10 bar gaseous oxygen from the cryogenic ASU (baseline process) is defined as:

$$\mu_{ox} = \left(\sum G_p - \sum D_{asu}\right) / Q_{in} \tag{4}$$

where,

$\sum G_p$ is the sum of the power generated from the supercritical steam power generation unit and the power from the cryogenic ASU air expander; $\sum D_{asu}$ is the sum of the power consumption by the air and gaseous oxygen compressors in the ASU as well as the pumps in the supercritical power generation unit and Q_{in} the thermal energy input into the system from the coal.

For Case 2, the efficiency of the standalone pressurized oxy-coal combustion process with pumped liquid oxygen to 10 bars is defined as:

$$\mu_{ox1} = \left(\sum G_p - \sum D_{asup}\right) / Q_{in} \tag{5}$$

where,

$\sum G_p$ is the sum of the power generated from the supercritical steam power generation unit and the power from the cryogenic ASU air expander; $\sum D_{asup}$ is the sum of the power consumption by the air compressors of ASU, liquid oxygen pump and the pumps in the supercritical power generation unit and Q_{in} is the thermal energy input into the system from the coal.

For case 3 where oxygen is pumped to 200 bars prior to vapourization in the main ASU heat exchanger followed by expanding to 10 bars, the efficiency is defined as:

$$\mu_{ox2} = \left(\sum G_{p2} - \sum D_{asup}\right) / Q_{in} \tag{6}$$

where,

$\sum G_{p2}$ is the sum of the power generated from the supercritical steam power generation unit, the power from the ASU air expander and the power from the oxygen expander; $\sum D_{asup}$ is the sum of the power consumption by the air compressors of ASU, liquid oxygen pump and the pumps in the supercritical power generation unit and Q_{in} is the heat input into the system from the fuel.

In Case 4, the efficiency improvement of Case 3 as a result of the recovery of the compressor waste heat using binary cycle heat engine is evaluated. In this case, the efficiency of the standalone pressurized oxy-coal combustion process with pumped oxygen to 200 bars prior to vapourization in the main ASU heat exchanger followed by expanding to 10 bars (i.e. Case 3) together with binary waste heat recovery from the ASU compressors is defined as:

$$\mu_{ox3} = \left(\sum G_{p3} - \sum D_{asupp}\right) \Big/ Q_{in} \quad (7)$$

where,

$\sum G_{p3}$ is the sum of the power generated from the supercritical steam power generation unit, the power from the ASU air expander, the power from the oxygen expander and the power from the binary cycle for heat recovery from ASU compressors; $\sum D_{asupp}$ is the sum of the power consumption by the air compressors of ASU, liquid oxygen pump, pumps in the supercritical power generation unit and the binary cycle pump and Q_{in} is the thermal energy input into the system from the fuel.

Case 5 focuses on the liquid air power generation unit of the entire process. The efficiency is defined as:

$$\mu_{la} = \left(G_{la} - D_{aux}\right) \Big/ \sum Q_{scp} \quad (8)$$

where,

G_{la} is the power generated from the liquid air power generation unit; D_{aux} is the discharging pump power consumption and $\sum Q_{scp}$ is the sum of the heat input into the system by the steam from the steam generation unit and the power consumption by the liquefaction compressor (i.e. the charging power).

In Case 6, the impact of the binary heat recovery from the charging compressor exhaust heat was investigated (i.e. Case 5 with heat recovery from the charging compressor exhaust heat using binary cycle heat engine). The efficiency of the liquid air power generation unit with binary cycle waste heat recovery from the compressors is given as:

$$\mu_{la1} = \left(\sum G_{la1} - \sum D_{aux1}\right) \Big/ \sum Q_{scp} \quad (9)$$

where,

$\sum G_{la1}$ is the sum of the power generated from the liquid air power generation unit and the binary cycle waste heat recovery from compressor; $\sum D_{aux1}$ is the sum of the pump power consumption by the liquid air power generation during the discharging operation and by the binary cycle engine pump and $\sum Q_{scp}$ is the sum of the heat input into the system by the steam from the steam power generation unit and the liquefaction process compression power.

In Case 7, the efficiency of the entire process is considered. The efficiency of the pressurized oxy-coal combustion process with pumped oxygen to 200 bars prior to vapourization in the main ASU heat exchanger followed by expanding to 10 bars integrated with liquid air power generation unit and binary cycle engine (i.e. Case 4 + Case 6) is defined as

$$\eta_{RT} = {(\sum G_{ov} - \sum D_{ov})}/{Q_{in}} \tag{10}$$

where,

$\sum G_{ov}$ is the sum of the power generated from the overall process except the inert expander This comprises of the power from the supercritical steam power generation unit, the liquid air power generation unit, the binary cycle waste heat recovery units (except those in the flue gas cleaning, CO_2 purification and compression unit), the oxygen expander, the air expander of the cryogenic ASU, $\sum D_{ov}$ is the sum of the power consumption by the auxiliary equipment such as pumps and ASU compressors except those in the flue gas cleaning, CO_2 purification and compression unit; $\sum Q_{in}$ is the sum of the thermal energy input from the coal and power consumption by the compressors of the liquefaction process (charging power consumption).

The corresponding efficiencies for the process with carbon capture is obtained by including the power generation and consumption in the flue gas cleaning, CO_2 purification and compression unit. This include: power generation in the inert expander, power generation in the binary cycle heat engines attached to the CO_2 compressor train exhaust and power consumption by the pumps and compressors.

4. Results and Discussions

The summary of the simulation results, stream conditions (mass flowrate, temperature and pressure) and the efficiency results for the different cases investigated in this work are shown in Tables 3, 4 and 5 respectively.

From Table 3, it can be seen that the oxygen purity generated from the ASU is about 95.68 mol% which met the requirement for a typical oxy-coal combustion process. The specific power consumption of the ASU is 0.309 kWh/kg-O_2, which is within the range of values quoted in the literature (Lombardi et al., 2011, Hong et al., 2009, Kansha et al., 2011). For a standalone pressurised oxy-coal process with gaseous oxygen compression to 10 bar (Case 1), the gross power generation from the supercritical steam power generation system was 572595.28 kW while the gross power consumption by the supercritical steam power generation unit pumps, gaseous oxygen compressor and cryogenic ASU compressors were 22821.52 kW, 20526.91 kW and 89094.10 kW respectively. This translates to an efficiency of 43.75% without carbon capture. The inclusion of carbon capture reduces the efficiency to 39.99% giving an energy penalty of 3.76%. Replacing the gaseous oxygen compressor with liquid oxygen pump (Case 2) increases the process efficiency to 45.79% and 42.03% for scenarios without and with carbon capture respectively. Case 3 shows that pumping the liquid oxygen to a pressure of 200 bars and expanding the gaseous oxygen to the required combustion pressure of 10 bars improved the efficiency by 0.66% and 2.7% respectively for processes with and without carbon capture when compared with processes with only liquid oxygen pump and gaseous oxygen compression.

Table 3: Summary of Simulation Results

Table 4: Stream Temperature, Pressure and Mass Flowrate

Table 5: Process Efficiencies

This is because more power is generated during oxygen expansion than is consumed during the pumping operation. For example, about 1603.21 kW of power was consumed in pumping the liquid oxygen to 200 bars while about 8182.53 kW of power is generated by expanding the high pressure gaseous oxygen to the required combustor pressure of 10 bars. The temperature of the oxygen stream changes from 20 ^oC before the expansion process to -139.50 ^oC after the expansion process. The exit oxygen from the expander is mixed with part of the recycled flue gas to obtain a stream at a temperature of 210 ^oC which is sent back to the combustion chamber. Although there is an improvement in process efficiency when Case 3 is compared with Case 2 and 1, doing this might not be economically attractive especially for Case 3 vs Case 2 since the improvement in efficiency of 0.66% might not be able to justify the cost of installing an additional oxygen expander. Case 4 shows the importance of recovering the waste heat from the compressor exhaust using binary cycle heat engine instead of the conventional water based inter-cooling/ after-cooling arrangement. The recovery of the compressor heat in the ASU adds a net power output of 9416.91 kW. The increase in the power translates to an increase in the efficiency to 47.38 % and 43.62% for cases without and with carbon capture.

Figure 8: P-h Diagram of R134a working fluid used in the ORC System attached to the Cryogenic ASU

In the same vein, cases 5 and 6 shows the efficiency of the liquid air power generation unit with and without waste heat recovery from the compressor exhaust stream using binary cycle heat engines. Without waste heat recovery, the efficiency of the liquid air power generation unit is 40.17%. This is improved to 42.69% when the waste heats from the compressors are converted to power using binary cycle heat engines. Figure 8 shows the Pressure-enthalpy diagram of the binary cycle heat engine (ORC) attached to the compressors in the cryogenic ASU. The flue gas cleaning, CO_2 purification and compression unit modeled in this work consumes about 38009.75 kW of power to generate 89.30 kg/s of CO_2 with purity of 95.35 mol.%. This gives a specific power consumption of 0.118 kWh/kg-CO_2. The round trip efficiency of the overall process is calculated as 56.01% and 54.74% for cases without and with carbon capture respectively. It is interesting to see that the round trip efficiency for the case with carbon capture is slightly lower than that without carbon capture. The reason is because, the sum of power obtained from the binary cycle waste heat recovery heat engines attached to the compressors in the flue gas cleaning, CO_2 purification and compression unit as well as the power from the inert expander is lower than the sum of the powers consumed by the compressors and pumps in the purification and compressor unit (39979.04 kW vs 26112.06 kW). Thus, with the use of binary waste heat recovery heat engines to convert the waste heat from the compressors used in the flue gas purification unit, it is possible to generate up to 65% of the power consumed in the flue gas cleaning, CO_2 purification and compression unit.

5. Conclusions

The study carried out in this paper shows that the integration of liquid air power generation process to a standalone pressurized oxy-coal supercritical steam power generation process brings an enormous thermodynamic advantage as seen by the increase in the thermodynamic efficiency of the integrated process when compared to the standalone process. The results also show that the recovery of the waste heat from the compressors using binary cycle heat engines also helps to improve the overall power generated from the process. It was also found that the power generated by the binary cycle heat engine which recovers waste heat from the entire compressor train of the flue gas cleaning, carbon dioxide purification and compressor unit is capable of offsetting up to 65% of the power required for the flue gas cleaning, carbon capture and compression process. The results also show the significance of incorporating waste heat recovery technology to recover compressor waste heat from processes which make use of compressors.

Acknowledgement

The authors would like to thank UK EPSRC (through EPSRC Capital Investment on Energy Storage) and University of Hull for their financial support.

References

ANEKE, M., AGNEW, B. & UNDERWOOD, C. (2011a) Approximate Analysis of the Economic Advantage of a Dual Source ORC System Over two Single ORC Systems in the Conversion of Dual low and Mid Grade Heat Sources. *Journal of EUEC,* 5**,** 1-17.

ANEKE, M., AGNEW, B. & UNDERWOOD, C. (2011b) Performance analysis of the Chena binary geothermal power plant. *Applied Thermal Engineering,* 31**,** 1825-1832.

ANEKE, M., AGNEW, B., UNDERWOOD, C., WU, H. & MASHEITI, S. (2012) Power Generation from Waste Heat in a Food Processing Application. *Applied Thermal Engineering,* 36**,** 171-180.

ANEKE, M. & WANG, M. (2015a) Improving the Energy Effficiency of Cryogenic Air Separation Unit (ASU) through Compressor Waste Heat Recovery using Direct Binary Heat Engine Cycle. IN GERNAEY, V. K., HUUSOM, K. J. & GANI, R. (Eds.) *12th International Symposium on Process Systems Engineering and 25th European Symposium on Computer Aided Process Engineering.* Copenhagen, Denmark, Elservier.

ANEKE, M. & WANG, M. (2015b) Potential for improving the energy efficiency of cryogenic air separation unit (ASU) using binary heat recovery cycles. *Applied Thermal Engineering,* 81**,** 223 - 231.

BARBUCCI, P. (2008) The Enel's CCS Project. *Enel - Engineering and Innovation Division- Italy*.

CASTLE, W. F. (2002) Air separation and liquefaction: recent developments and prospects for the beginning of the new millennium. *International Journal of Refrigeration,* 25**,** 158 - 172.

CIFERNO, J. P., FOUT, T. E., JONES, A. P. & MURPHY, J. T. (2000) Capturing Carbon from Existing Coal-Fired Power Plants. *American Institute of Chemical Engineers,* April**,** 33 - 41.

HAGI, H., NEMER, M., LE MOULLEC, Y. & BOUALLOU, C. (2013) Assessment of the Flue Gas Recyle Strategies on Oxy-Coal Power Plants using an Exergy-based Methodology. *Chemical engineering Transactions,* 35**,** 343 - 346.

HONG, J., CHAUDHRY, G., BRISSON, J. G., FIELD, R. & GAZZINO, M. (2009) Anaysis of oxy-fuel combustion power cycle utilizing a pressurized coal combustor. *Energy,* 34**,** 1332 - 1340.

HU, Y. & YAN, J. (2011) Characterization of flue gas in oxy-coal combustion processes for CO_2 capture. *Applied Energy,* 90**,** 113 - 121.

IEA (2011) CO_2 Emissions from fuel combustion: Highlights. *International Energy Agency*.

IEA (2012) Key World Energy Statistics. *International Energy Agency,* www.iea.org.

IEA (2013) Key World Energy Statistics. *International Energy Agency*.

KANSHA, Y., KISHIMOTO, A., NAKAGAWA, T. & TSUTSUMI, A. (2011) A novel cryogenic air separation process based on self-heat recuperation. *Separation and Purification Technology,* 77**,** 389 - 396.

LOMBARDI, L., CARNEVALE, E. & CORTI, A. (2011) Analysis of energy recovery potential using innovative technologies of waste gasification. *Waste Management,* 32**,** 640 - 652.

MANENTI, F., ROSSI, F., CROCE, G., GROTTOLI, M. G. & ALTAVILLA, M. (2013) Intensifying Air Separation Units. *Chemical engineering Transactions,* 35.

ROY, B. & BHATTACHARYA, S. (2013) Oxy-fuel Combustion Performance of Victorian Brown Coals in a 10 kW_{th} Fluidized Bed. *3rd Oxyfuel Combustion Conference.* Ponferrada, Spain.

RÜBBERDT, K. (2009) Producing oxygen and nitrogen: Air separation techniques continue to advance. *ACHEMA 2009, 29th International Exhibition Congress in Chemical Engineering, Environmental Protection and Biotechnology.* Frankfurt am Main, Germany.

STRAHAN, D. (2013) Liquid Air Technologies - a guide to potential. *Centre for Cryogenic Energy Storage, University of Birmingham, UK.*

TSUKAHARA, H., ISHIDA, T. & MAYUMI, M. (1999) Gas-Phase Oxidation of Nitric Oxide: Chemical Kinetics and Rate Constant. *Ideal,* 3**,** 191 - 198.

WCA (2014) Coal & Electricity. World Coal Association, Available at: www.worldcoal.org, Accessed 29th October: 2014.

WHITE, V., TORRENTE-MURCIANO, L., STURGEON, D. & CHADWICK, D. (2009) Purificatin of Oxyfuel-Derived CO_2. *Energy Procedia,* 1**,** 399 - 406.

ZHENG, L. (Ed.) (2011) *Oxy-Fuel Combustion for Power Generation and Carbon Dioxide (CO_2) Capture*, Woodhead, UK.

Figure

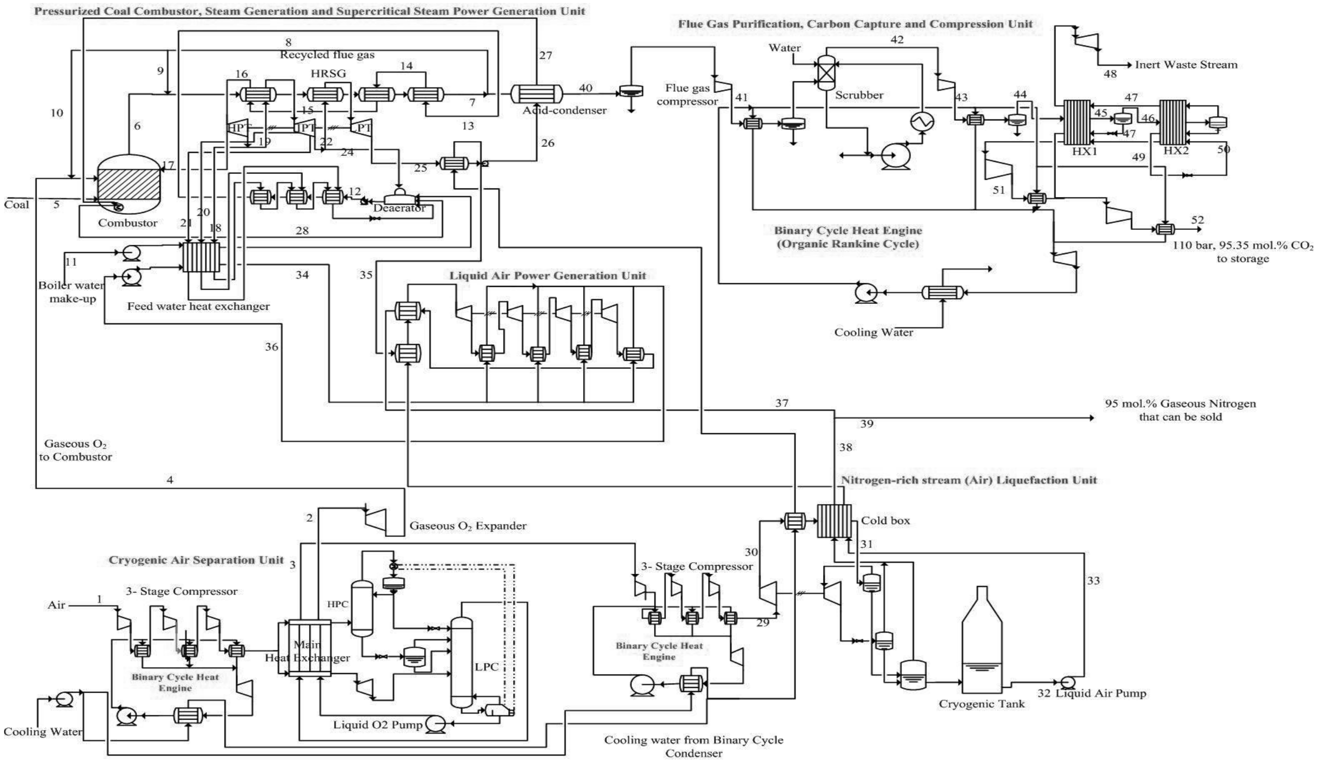

Figure 1: Overall Process Flow Diagram of the Pressurized Oxy-coal Power Cycle for Carbon Capture Application Integrated with LAPG and Binary Cycle Engine

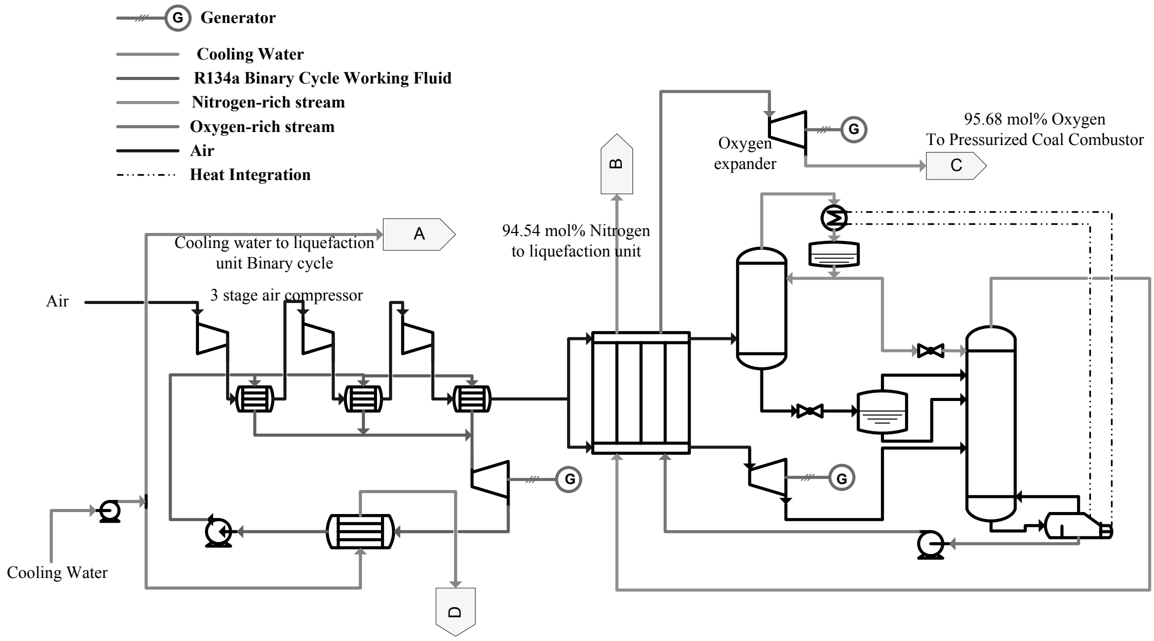

Figure 2: Process Flow Diagram of Cryogenic ASU

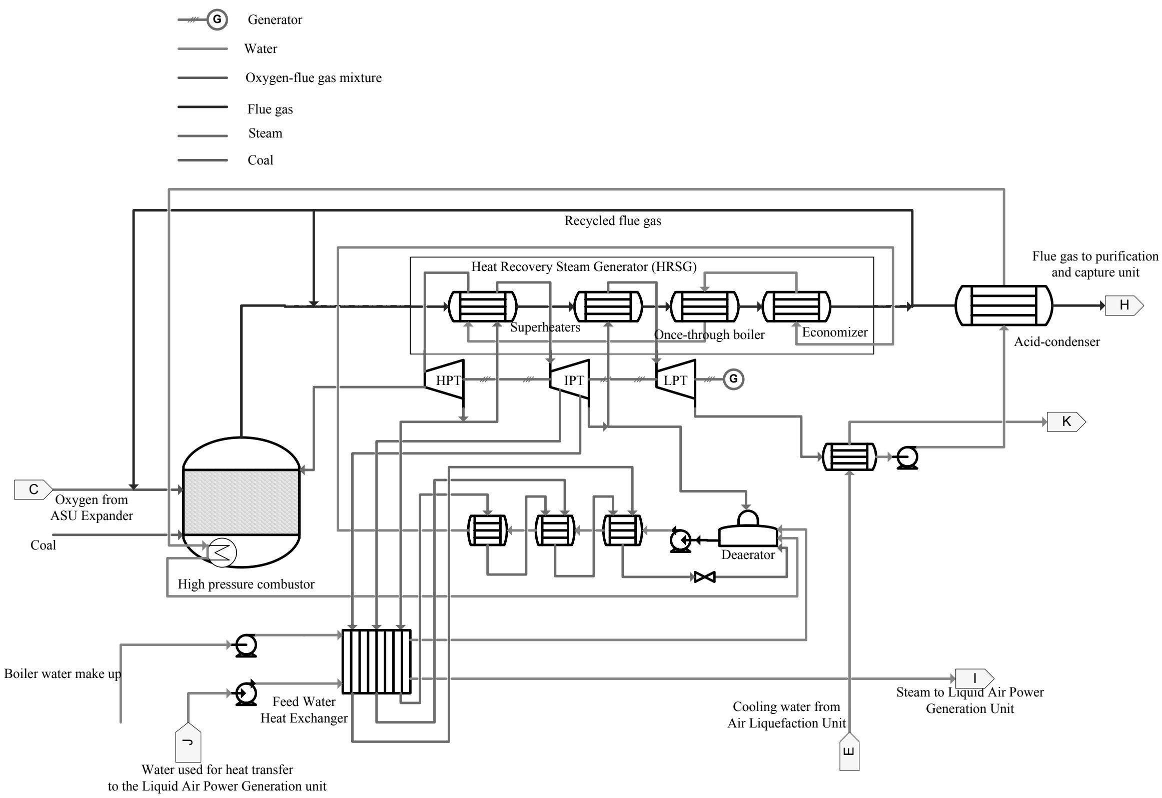

Figure: 3 Process Flow Diagram of Pressurized Combustor Unit, Steam Generation Unit and Supercritical Steam Power Generation Unit

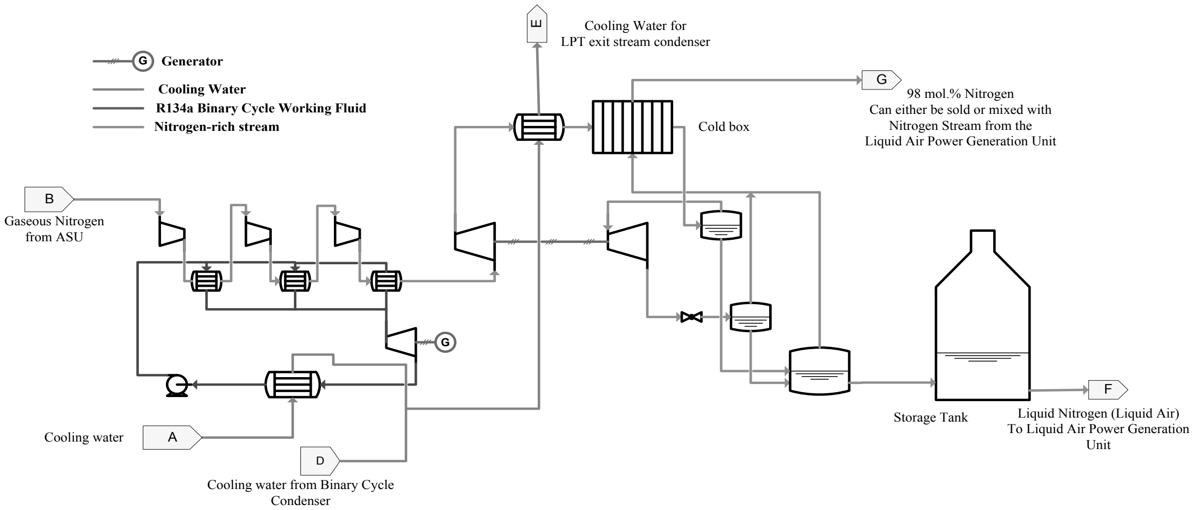

Figure 4: Process Flow Diagram of Air Liquefaction Unit

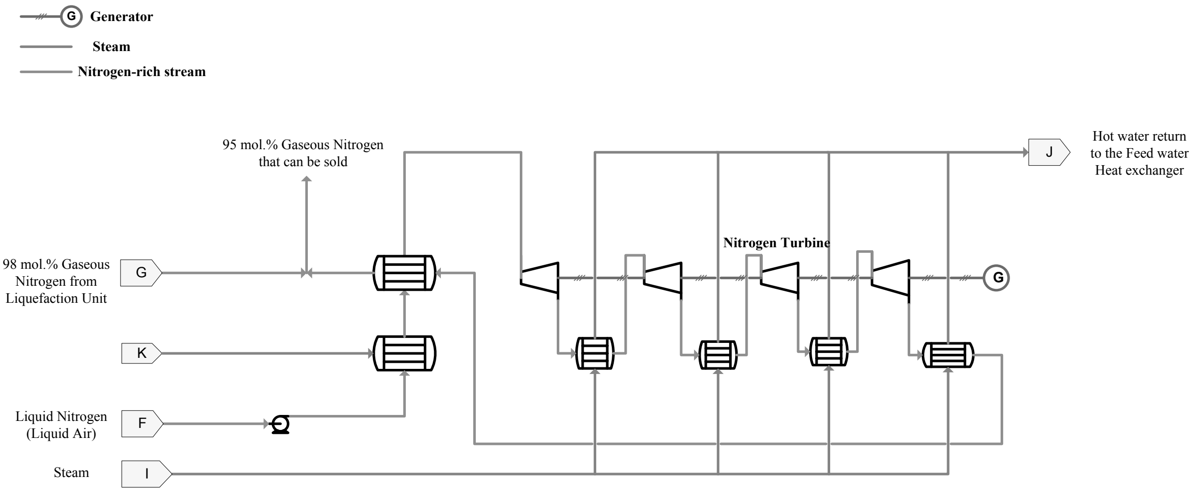

Figure 5: Liquid Air Power Generation Unit

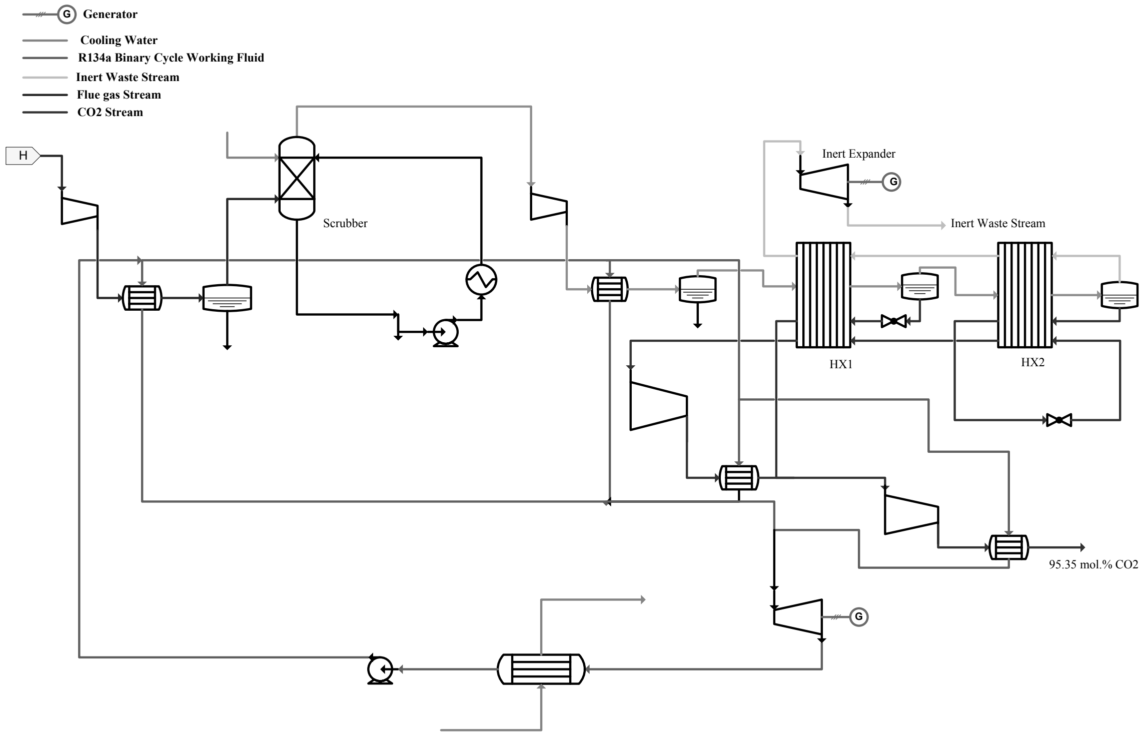

Figure 6: Process Flow Diagram of flue gas Cleaning, CO_2 purification and compression unit

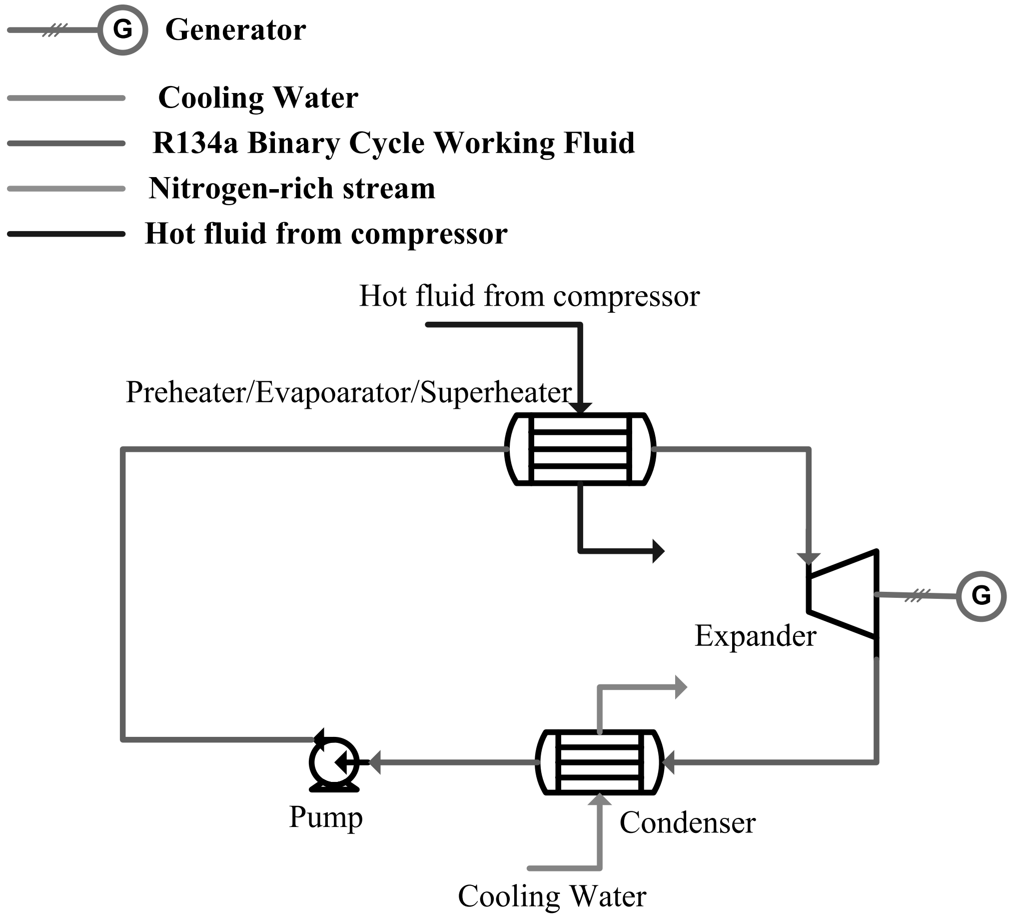

Figure 7: Process Flow Diagram of Organic Rankine Cycle

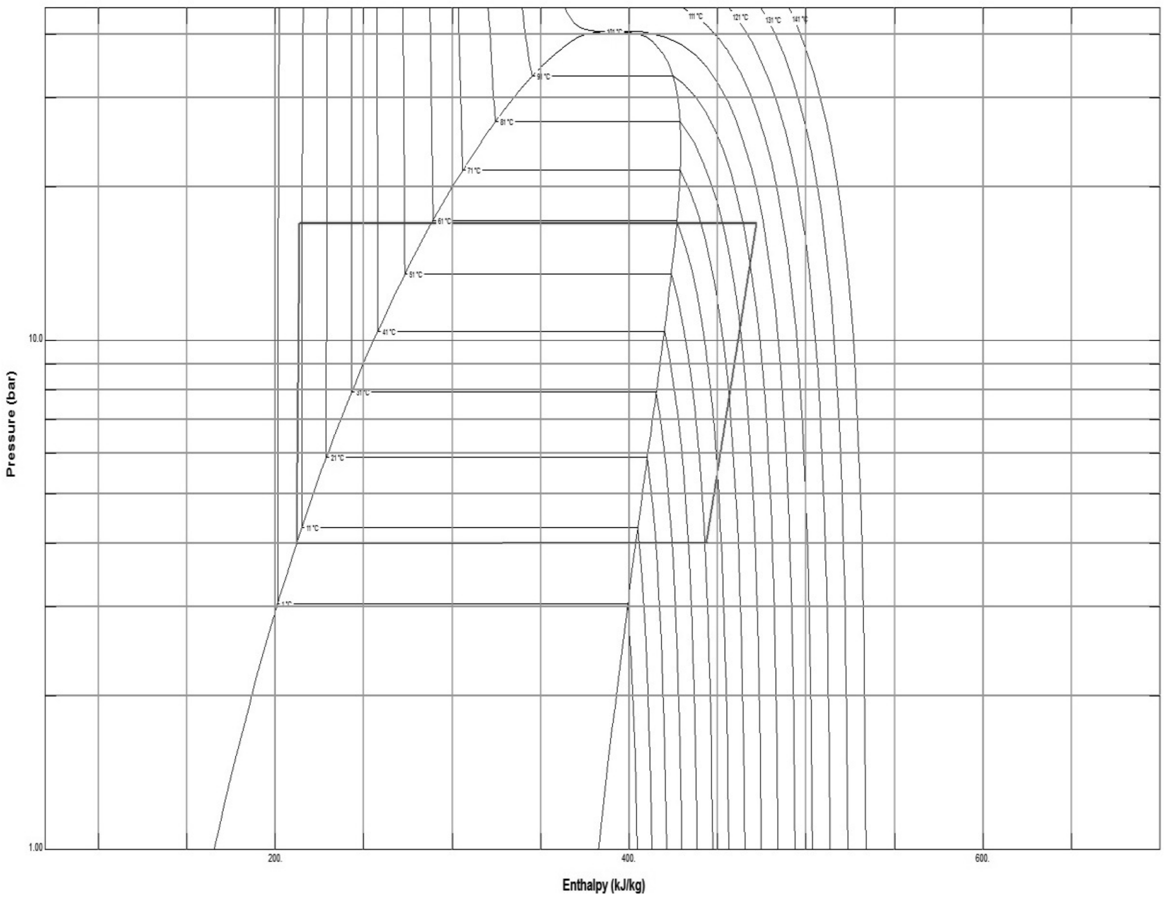

Figure 8: P-h diagram of R134a used in the ORC system attached to the Cryogenic ASU

Tables

Table 1: Properties of coal used in the simulation (adapted from (Hu and Yan, 2011))

Coal Type	**Bituminous**
Moisture (wt.%) as analysed	1.07
Proximate (wt.%) (dry)	
Ash	8.75
Volatile matter	35.33
Fixed carbon	54.85
Ultimate (wt.%) (dry)	
Carbon	77.65
Hydrogen	5.04
Nitrogen	1.49
Sulfur	0.95
Ash	8.84
Oxygen	6.03
Heating value (MJ/kg)	32.51

Table 2: Process Simulation Parameters

Parameters	Value
Cryogenic ASU	
Air mass flowrate	400 kg/s
Air composition (mol. %)	
Nitrogen	78.12
Oxygen	20.95
Argon	0.93
Compressor discharge pressure	6.35 bar
LPC Pressure	1.2 bar
HPC Pressure	5.7 bar
No of stages in LPC	69
No of stages in HPC	45
Liquid oxygen pump discharge pressure	200 bar
Gaseous oxygen expander inlet pressure	200 bar
Pressurized Oxy-Coal Process	
Coal mass flowrate	31.11 kg/s
Combustor pressure	10 bar
Combustor temperature	1550 ^{o}C
Steam Generation Unit	
Flue gas inlet temperature to HRSG	730 ^{o}C
Flue gas outlet temperature from HRSG	239 ^{o}C
Supercritical Power Generation Unit	
Turbine inlet pressure	250 bar
Turbine inlet temperature	600 ^{o}C
Reheat Temperature	620 ^{o}C
Deaerator Pressure	10 bars
Air Liquefaction Unit	
Compressor discharge pressure	8 bars
Liquid air temperature	-189 ^{o}C
Liquid air Pressure	1.99 bars
Liquid Air Power Generation Unit	
Turbine inlet pressure	120 bars
Reheat temperature	70 ^{o}C
Flue Gas Cleaning, CO_2 purification and compression unit	
Inert expander inlet pressure	30 bars
Overall Process	
Pump efficiency	0.80
Compression efficiency	0.80
Turbine Efficiency	0.80

Table 3: Summary of Simulation Results

Performance Parameters	Value
Cryogenic ASU	
Materials	
Oxygen stream mass flowrate (kg/s)	78.01
Oxygen stream composition (mol. %)	
Nitrogen	0.80
Oxygen	95.68
Argon	3.52
Nitrogen-rich stream mass flowrate (kg/s)	321.99
Nitrogen-rich stream composition (mol. %)	
Nitrogen	94.54
Oxygen	5.08
Argon	0.38
Power Consumption & Generation (kW)	
Compressor Power consumption	89094.10
Liquid Oxygen Pump power consumption	1603.21
Gaseous Oxygen Expander Power output	8182.53
Air Expander Power output	2340.59
Supercritical Power Generation Unit (kW)	
Gross Turbine Power output	572595.28
Gross Pump Power consumption	22821.52
Air (Nitrogen-rich stream) Liquefaction Unit Power Consumption (kW)	
Compressor Power Consumption (Charging Power)	78219.00
Liquid Air Power Generation Unit	
Liquid Air Pump Power consumption (kW)	5048.40
Liquid Air Turbine Power output (kW)	125908.31
Thermal Energy Input from steam for Liquid Air Vapourization (kW_{th})	222639.45
Flue Gas Cleaning, Carbon dioxide purification and Compression Unit	
Flue gas purification and CO_2 compression train power consumption (kW)	37989.27
Scrubber recirculating stream pump power consumption (kW)	204.77
Inert Expander Power generation (kW)	184.29
CO_2 stream purity (mol. %)	95.35
CO_2 stream mass flowrate (kg/s)	89.30
Binary Cycle Heat Engine Power (kW)	
ASU compressor heat recovery binary cycle power output	9860.37
ASU binary cycle pump power consumption	443.46
Liquefaction compressor heat recovery binary cycle power output	7978.31
Liquefaction binary cycle pump power consumption	406.62
Flue gas purification and CO_2 compression binary cycle power output	25927.77
Flue gas purification and CO_2 compression binary cycle pump power consumption	1785.00

Table 4: Stream Temperature, Pressure and Mass Flowrate

Stream no	Mass flowrate (kg/s)	Pressure (bar)	Temperature (^oC)
1	400.00	1.01	30.00
2	78.01	200.00	20.00
3	321.99	1.10	20.00
4	78.01	10.00	-139.50
5	31.11	10.00	25.00
6	803.85	10.00	1550.00
7	2106.73	10.00	239.07
9	1602.88	10.00	239.07
10	563.18	10.00	239.07
12	657.78	250.00	184.46
13	657.78	250.00	215.00
16	657.78	250.00	600.00
18	105.24	50.00	340.59
19	420.98	50.00	340.59
22	188.60	10.00	384.85
25	188.60	0.41	232.18
26	188.60	11.20	32.96
30	321.99	11.77	64.40
31	321.99	11.77	-163.00
32	289.15	1.99	-189.00
33	289.15	120.00	-184.08
40	240.67	10.00	167.19
41	199.69	15.00	217.91
42	92.03	15.00	26.05
43	92.03	30.00	86.93
44	91.95	30.00	40.00
45	91.95	30.00	-10.00
46	55.88	30.00	-10.00
47	2.70	30.00	-20.00
48	2.70	7.00	-61.94
49	53.17	30.00	-20.00
50	53.17	5.00	-61.52
51	53.17	20.00	161.41
52	89.24	110.00	37.78

Table 5: Process Efficiencies

Performance Parameters	Case 1	Case 2	Case 3	Case 4	Case 5	Case 6	Case 7
Q_{in}	1011386.10[a,b]	1011386.10[a,b]	1011386.10[a,b]	1011386.10[a,b]			1089605.10[a,b]
$\sum Q_{scp}$					300858.45	300858.45	
$\sum G_{P}$	574935.87[a] 575120.16[b]	574935.87[a] 575120.16[b]					
$\sum G_{P2}$			583118.40[a] 583302.69[b]				
$\sum G_{P3}$				592978.77[a] 593163.06[b]			
G_{la}					125908.31		
$\sum G_{ov}$							724524.80[a] 750636.86[b]
$\sum G_{la1}$						133886.62	
$\sum D_{asu}$	132442.53[a] 170636.57[b]						
$\sum D_{asup}$		111847.11[a] 150041.15[b]	113379.74[b] 151573.78[b]				
$\sum D_{asupp}$				113823.20[a] 152017.24[b]			
D_{aux}					5048.40		
$\sum D_{aux1}$						5455.02	
$\sum D_{ov}$							114229.83[a] 154208.87[b]
Efficiency	μ_{ox}	μ_{ox1}	μ_{ox2}	μ_{ox3}	μ_{la}	μ_{la1}	η_{RT}
	43.75%[a] 39.99%[b]	45.79%[a] 42.03%[b]	46.45%[a] 42.69%[b]	47.38%[a] 43.62%[b]	40.17%	42.69%	56.01%[a] 54.74%[b]

All parameters are in kW; (a) means without carbon capture; (b) means with carbon capture